

Synthesis and Photocatalytic Properties of Sol-Gel Derived B_2O_3 - SiO_2 - TiO_2 Glass-Ceramic Coatings

Yasser MoradHaseli¹, Bijan Eftekhari Yekta¹, Alireza Mirhabibi², Sara Ahmadi^{3,*}

* s.ahmadi@standard.ac.ir

¹ Ceramic Division, School of Materials and Metallurgy Engineering, Iran University of Science and Technology, Tehran, Iran

² School of Chemical and Process Engineering, University of Leeds, Leeds, LS2 9JT

³ Construction and Minerals Research Group, Technology and Engineering Research Center, Standard Research Institute, Karaj, Alborz, Iran

Received: January 2025

Revised: June 2025

Accepted: August 2025

DOI: 10.22068/ijmse.3885

Abstract: The crystallization behavior and photocatalytic properties of the sol-gel derived glass ceramic coatings in the TiO_2 - SiO_2 - B_2O_3 system were studied. The prepared solution was sprayed onto a glazed ceramic wall. Following drying, the coated specimens were fired at 900°C for 1h. The impact of boron oxide content in the composition was explored in terms of anatase stability and glass maturing temperature. The thermal and crystallization behaviors of the dried gels were investigated using STA, XRD, and FESEM. The photocatalytic property of the coated layer was examined using the degradation of methylene blue. Based on the results, the sample containing 15 wt% boron oxide demonstrated approximately 30% dye removal efficiency after only 60 min of UV irradiation. Additionally, this particular sample exhibited the greatest magnitude of the anatase phase in comparison to the other samples.

Keywords: Sol-gel, Photocatalyst, Glass-ceramic coating, Anatase.

1. INTRODUCTION

Nowadays, air and water pollution have become among the most critical environmental challenges. One promising solution involves the use of photocatalytic materials such as TiO_2 , ZrO_2 , ZnO , and CdS [1]. Among these, titanium dioxide (TiO_2) stands out due to its strong oxidation potential and remarkable hydrophilicity, which enable its applications in air purification, deodorisation, sterilisation, and self-cleaning surfaces [2, 3]. In contrast, alternative systems such as ZnO , while possessing similar band gaps to TiO_2 , suffer from photocorrosion under UV irradiation. CdS , another potential candidate, is limited by its toxicity and instability under light exposure. ZrO_2 , although chemically stable, has a wider band gap, which reduces its photocatalytic efficiency under UV light [1-3].

The photocatalytic performance of TiO_2 is influenced by several factors, including its crystal structure, morphology, surface area, porosity, and pore distribution [4-6]. TiO_2 occurs in three polymorphs: brookite, anatase, and rutile. While anatase demonstrates the highest photocatalytic activity, it irreversibly transforms to rutile at temperatures between 500–600°C [3-5].

To enhance the performance and stability of TiO_2 , numerous studies have focused on modifications, including doping and the use of fluxing agents. For example, Jung et al. demonstrated that B_2O_3 flux improves TiO_2 crystallinity while preserving the anatase phase [7], a finding supported by other researchers [8, 9]. Additionally, incorporating silica has been shown to enhance both the thermal stability of the anatase phase and its photocatalytic efficiency [1, 3, 10–14].

Resende et al. [15] demonstrated that TiO_2 / SiO_2 - B_2O_3 ternary nanocomposites exhibit superior photocatalytic activity compared to commercial TiO_2 , attributing this enhancement to the unique interfacial properties introduced by B_2O_3 . Furthermore, Bachvarova-Nedelcheva et al. [16] reported that the inclusion of B_2O_3 in TiO_2 -based systems not only stabilises the anatase phase but also imparts antibacterial properties, expanding the material's applicability. Consequently, the B_2O_3 - SiO_2 - TiO_2 system was selected for this study due to its synergistic properties, which enhance photocatalytic performance and offer a balanced combination of stability, safety, and improved photocatalytic performance, making it a superior choice for environmental applications. A critical factor in practical applications is the

durability of photocatalytic TiO_2 coatings. Conventional coatings often exhibit weak adhesion to glazed surfaces, which limits their longevity. In contrast, TiO_2 -based glass-ceramic layers have exhibited superior bonding and durability. The enhanced adhesion and durability of TiO_2 -based glass-ceramic coatings, compared to conventional TiO_2 layers, can be attributed to several interrelated factors. First, the glass-ceramic matrix enables the formation of strong chemical bonds (e.g., Si-O-M and Ti-O-M , where M is a metal from the substrate) at the interface with the glazed substrate, which significantly surpasses the weak van der Waals interactions typical of conventional coatings. Moreover, the coefficient of thermal expansion (CTE) of glass-ceramic systems can be tailored to match that of the glazed surface more closely, thereby reducing thermal mismatch stress during firing and cooling. Additionally, partial softening of the glassy phase during sintering enables mechanical interlocking, as the coating partially penetrates surface irregularities, thereby anchoring it more securely. Furthermore, the in-situ crystallization of nanometric anatase crystals within the glassy matrix improves the mechanical stability and resistance to cracking or delamination. Ultimately, the embedding of TiO_2 particles in a glassy network offers environmental protection, particularly against moisture and UV-induced degradation, thereby enhancing long-term performance. These synergistic effects, as supported by references [17] and [18], explain the superior bonding strength and durability observed in glass-ceramic TiO_2 coatings.

TiO_2 also serves as a nucleating agent in the fabrication of glass ceramics, facilitating controlled crystallization and enabling the production of materials with desirable crystallite sizes and microstructures [19]. These glass ceramics are valued for their cost-effectiveness, ease of shaping, and versatility in various forms, including sheets, rods, tubes, and fibres, making them suitable for photocatalytic applications.

Recent research has explored TiO_2 -containing glass ceramics as photocatalytic materials. For instance, Yazawa et al. synthesized rutile-type glass ceramics from silicate glasses [20-21], while other studies have successfully derived anatase-type glass ceramics from phosphate glasses [22]. These materials exhibited photocatalytic activity, as evidenced by the degradation of methylene blue under UV light [23].

In this study, anatase-phase TiO_2 was precipitated within a SiO_2 - TiO_2 - B_2O_3 glass layer via heat treatment of sol-gel-derived glass. The photocatalytic activity of the resulting glass-ceramic layer was quantitatively evaluated.

2. EXPERIMENTAL PROCEDURES

2.1. Materials and Sample Preparation

the borosilicate glasses in the SiO_2 - B_2O_3 - TiO_2 system were prepared with sol gel method from reagent grade chemicals consisted of tetraethyl orthosilicate (TEOS, $(\text{Si}(\text{OC}_2\text{H}_5)_4)$, Merck 800658), Titanium tetraisopropoxide (TTIP, $\text{Ti}(\text{Opri})_4$, Merck 8251895), trimethyl borate $(\text{B}(\text{OCH}_3)_3)$, Merck 82180), isopropanol (IPA, Merck 109634), ethanol (EtOH , Merck 100983); Hydrochloric acid (37% solution, Merck 100317), and deionized water.

The nominal chemical compositions of the synthesised glass-ceramics are presented in Table 1.

Table 1. The nominal chemical compositions (wt.%) of the glasses

Composition	SiO_2	B_2O_3	TiO_2
ST-5B	30	5	65
ST-10B	30	10	60
ST-15B	30	15	55

Preparation of the sols was initiated by dissolution of TEOS in ethanol (1:4 molar ratios) and TTIP in isopropanol (1:4 molar ratios). The Si and Ti alkoxides hydrolysed by adding 1 M HCl as a catalyst. Following a 2h stirring, the solution of Ti-tetraisopropoxide in isopropanol was added dropwise to the TEOS sol. The resulting solution was stirred until a transparent and solid-free solution was achieved. Then, trimethyl borate with a stoichiometric amount of water was added to the alkoxide solution.

To ensure thorough hydrolysis of the alkoxides, the water content of the final solution was raised to twice the stoichiometric quantity and then agitated for 3h. The final Titania-Silica-Borate sols were completely transparent without any precipitation. The prepared sols were applied to the glazed ceramic tile by a spraying process. The coated tiles were dried at 150°C for 24h and then heat-treated at various temperatures to prepare glass ceramic. The heating rate was $10^\circ\text{C}/\text{min}$. Fig. 1 depicts the flowchart of the gel preparation procedure.

Methylene blue (MB, 159270) with chemical

formula $C_{16}H_{18}ClN_3S.nH_2O$ ($n=2-3$) was employed as the representative pollutant to study the photocatalytic properties of the prepared glass-ceramic layers coated on the glazed ceramic tiles.

2.2. Characterization Techniques

The thermal behaviour of the dried gels was studied using Simultaneous Thermal Analysis (STA, TA Instruments Q600) in both air and argon atmospheres. The heating rate was set at $10^\circ\text{C}/\text{min}$, and the temperature ranged up to 900°C .

The crystallinity and the average crystallite size were determined by the X-ray diffraction technique with Cu $K\alpha$ wavelength at 30 mA and 40 kV (XRD Bourestnik Dron-8).

The microstructure of the resulting glass-ceramic coating layer was characterised by field emission scanning electron microscopy (FESEM, Mira 3-XMU) and scanning electron microscopy (SEM, TESCAN VWGAI) with an accelerating voltage of 15-20 kV. The surface of the samples was etched in a 5% HF solution for 40 seconds before the test. The photo-degradation of a Methylene Blue aqueous solution was measured to assess the photocatalytic activity. The initial pollutant concentration was 10 micromolar, and the UV source irradiated the coated layer.

The MB removal efficiency was calculated by applying Eq. (1):

$$\text{Removal efficiency (\%)} = [(C_0 - C)/C_0] \times 100 \quad (1)$$

Where C_0 and C are the initial and residual MB concentrations in the feed solution, respectively. Before the experiment, the sample was stored in a dark environment. Subsequently, the samples were exposed to radiation for 1 hour, and their absorbance was measured using a UV-Vis spectrophotometer (PerkinElmer, Lambda 25) during this period.

3. RESULTS AND DISCUSSION

3.1. Thermal Analysis of the Sample

Figure 2 depicts the STA result of the dried ST-15B sample, taken in the air flow atmosphere. Two distinct endothermic peaks on the DTA thermograph, at approximately 70°C and 190°C , correspond to two weight reductions in the Tg thermograph. The observed endothermic peaks can be ascribed to the evaporation of mechanical water and rigid water from the sample. An exothermic peak occurring at approximately 270°C is attributed to the oxidation of carbon groups. Moreover, since the test was conducted on the gel before the heat treatment of the samples, there is no discernible peak reflecting crystallisation.

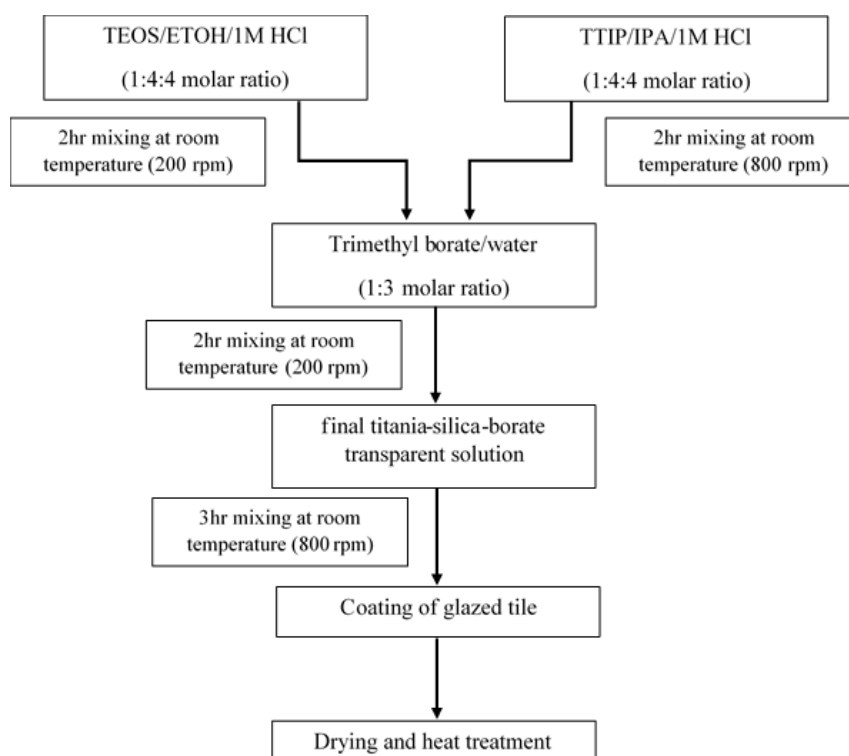


Fig. 1. The flowchart of the glass ceramic coating preparation procedure

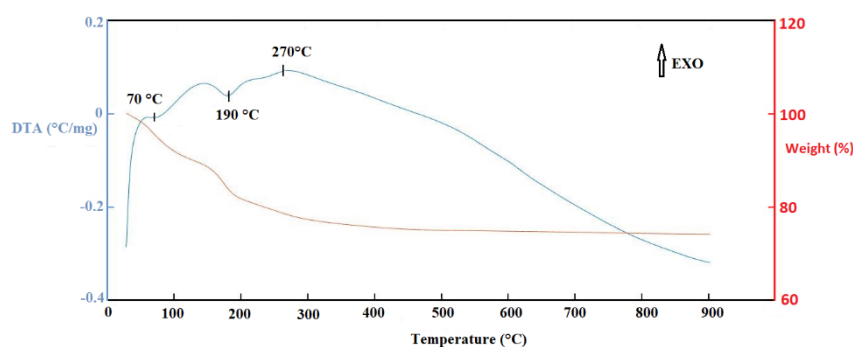


Fig. 2. STA results of sample ST-15B in an air atmosphere

3.2. Crystallisation Behaviour

Figure 3 displays the X-ray diffraction (XRD) patterns of prepared samples following a 24-hour drying period at 150°C. The observed pattern indicates that the dried gel exhibits an amorphous structure.

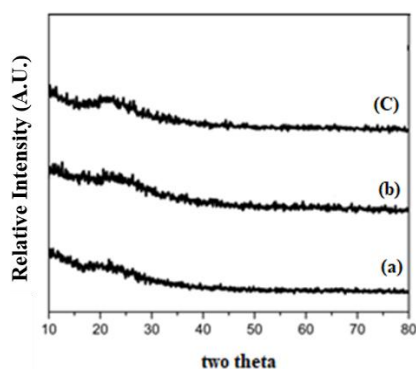


Fig. 3. XRD pattern of the a) ST-5B, b) ST-10B and c) ST-15B after drying at 150°C for 24h

Fig. 4 presents the XRD patterns of sample ST-15B after calcination at 150°C, 300°C and 400°C for 1h. According to the figure, anatase formed in the gel, and crystallisation increased as the temperature increased. The sample contains no evidence of rutile or brookite following the heat-treatment technique described above. The anatase phase peaks around $2\theta=25.3^\circ$ became sharper and more intense as the boron level increased.

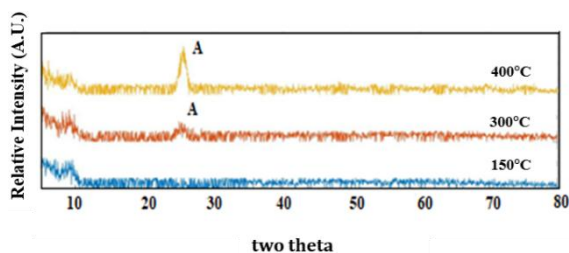


Fig. 4. XRD patterns of the ST-15B sample calcination at different temperatures. A: anatase

It should be noted that adding B_2O_3 to the coating composition instead of TiO_2 decreases the sintering temperature of the coating [4]. Furthermore, it is claimed that adding boron to the crystalline structure of TiO_2 enhances the thermal stability of anatase [5, 6]. The sintering of the layer improved with increasing boron oxide concentration, while the coating's crystallinity steadily increased, despite a gradual reduction in titanium oxide content within the coated layer. The XRD results, as shown in Figure 5, indicate that the addition of B_2O_3 to the TiO_2 system inhibits crystal growth and stabilises the anatase phase, even at elevated temperatures. This behaviour is consistent with previous findings in the literature and confirms the importance of boron in the stability of anatase. Mulmi et al. [24] reported that boron doping suppresses the growth of anatase crystals and maintains phase stability, as evidenced by their XRD patterns at room temperature. Similarly, Quesada-González et al. [25] found that the presence of boric acid during TiO_2 synthesis inhibited the rutile phase formation and promoted anatase phase stability.

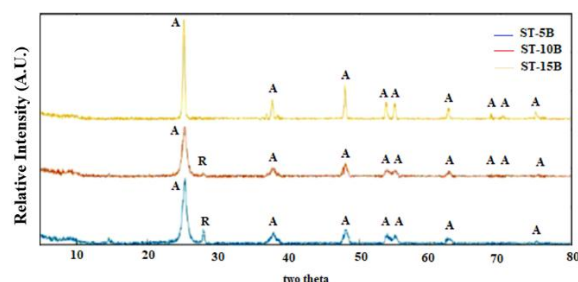


Fig. 5. The XRD pattern of samples after firing at 900°C for 1h

The crystallite size, lattice parameters, and the amounts of phases in the glass-ceramic layers fired at 900°C were determined using the Scherrer equation [5] and Rietveld refinement via Maud

software. The statistical parameter SIG, which reflects the quality of the fit in the refinement, is also reported for each sample (Table 2).

The results show that by increasing the amounts of boron oxide from 5 to 15 wt%, both the crystallite size and the quantity of anatase have increased. Previous studies have reported that the highest photocatalytic activity of an anatase coating occurs with a crystallite size in the range of 8-10 nm, which is achieved after calcination at temperatures below 500°C. In this study, however, the size of the crystals has increased due to the force to increase the firing temperature of the coated layer. After considering all the criteria, sample ST-15B was selected for further study due to its high concentration of anatase crystalline phase and excellent surface quality following firing at 900°C.

3.3. Microstructural Studies

Figure 6 depicts the FESEM images of the top views of the ST-15B glass-ceramic coated layer after being fired at 900°C for 1 hour. Surfaces with roughness and particles with uneven boundaries are detected. The coarse textures are a product of the HF etching procedure, which

eliminates the remaining glassy phase and exposes more crystal particles on the surfaces. Due to their greater specific surface areas, this surface shape is considered advantageous for enhancing photocatalytic activity. The image shows that the anatase crystalline size is less than 65 nm, which accurately corresponds to the findings in Table 2.

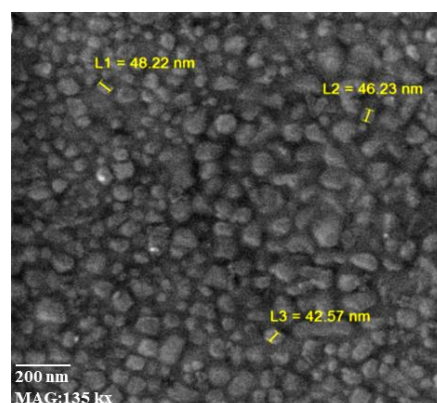


Fig. 6. SEM micrographs of the ST-15B glass-ceramic

The cross-sectional view of the glaze-coated layer ST-15B interface is displayed in Figure 7.

Table 2. The crystallite size, unit cell dimensions, and the estimated amounts of various phases of the samples after firing at 900°C

Sample	SIG	Phase	Unit Cell(A)		Quantity of phases (wt.%)	The crystallite size (nm)
			a	C		
ST-5B	1.5054	Anatase	3.78	9.49	38	20
		Rutile	4.55	2.90	2	100
		Amorphous	-	-	60	-
ST-10B	1.4012	Anatase	3.79	9.51	54	21
		Rutile	4.55	2.90	1.5-2	100
		Amorphous	-	-	44	-
ST-15B	1.6494	rutile	-	-	0	-
		Anatase	3.77	9.53	65	53
		Amorphous	-	-	35	-

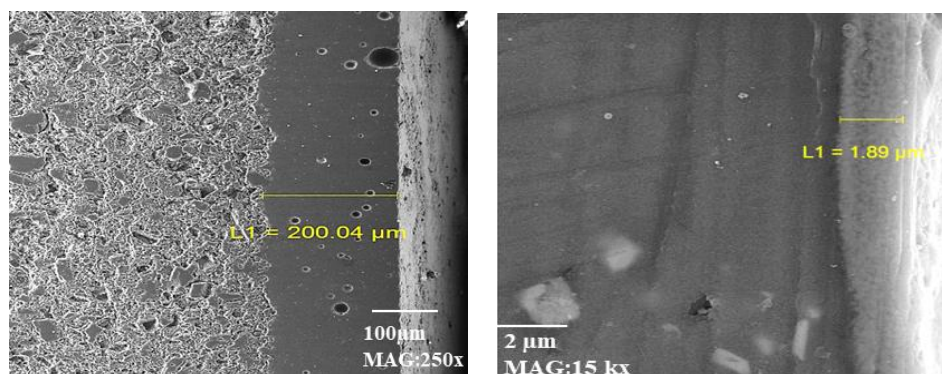


Fig. 7. Cross-section of Photocatalyst-coated glazed tile with ST-15B composition

As can be observed, the coating exhibits good adhesion to the glaze. From these figures, the thickness of the glaze and photocatalytic coatings are estimated to be 200 μm and 1.89 μm , respectively. These thicknesses are considered sufficient for coatings with satisfactory endurance.

3.4. Photocatalytic Properties

The photocatalytic properties of the samples were assessed by measuring the change in absorbance of the MB solution under UV radiation after exposure for 15 to 60 minutes, as depicted in Figure 8.

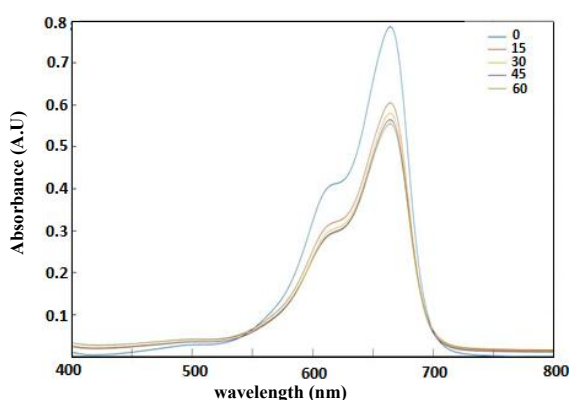
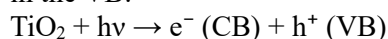


Fig. 8. Absorbance curves of MB aqueous solution in the presence of the ST-15B glass ceramic after UV-radiation

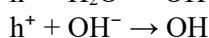
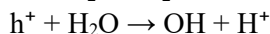
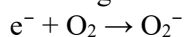
According to the colour degradation curve, the degradation efficiency has improved with increasing radiation time. Actually, absorption decreases throughout the 60 minute course, and the degradation and decolourization process nears completion.

The photocatalytic activity observed in our study is primarily attributed to the anatase phase of TiO_2 , which is well-known for its superior photocatalytic properties compared to the rutile and brookite phases. Anatase has a suitable band gap (~ 3.2 eV) that allows efficient absorption of UV light, resulting in the generation of electron-hole pairs (e^-/h^+) upon irradiation. Once excited, electrons in the valence band (VB) are promoted to the conduction band (CB), leaving behind holes in the VB:



These charge carriers can migrate to the surface of the catalyst, where they participate in redox reactions. The photogenerated electrons reduce dissolved oxygen molecules to superoxide radicals (O_2^-), while the holes oxidize water or hydroxide

ions to generate hydroxyl radicals ($\text{OH}\cdot$):



Both superoxide and hydroxyl radicals are highly reactive species capable of attacking and degrading organic dye molecules such as methylene blue into non-toxic byproducts like CO_2 and H_2O [26-27].

However, the photocatalytic efficiency can be affected by the recombination of e^-/h^+ pairs, which reduces the number of charge carriers available for surface reactions. Furthermore, the presence of other ions or compounds in solution can scavenge reactive species, leading to decreased degradation efficiency. As previously stated, the photocatalytic activity of the coating depends on the crystallinity and size of the anatase crystals. Consequently, etching the glass ceramic before radiation can enhance the photocatalytic activity of the synthesised coatings.

4. CONCLUSIONS

A single-phase transparent glass ceramic coating with photocatalytic properties was successfully synthesised by heat treatment of sol-gel derived specimens in the $\text{TiO}_2\text{-B}_2\text{O}_3\text{-SiO}_2$ system. The following conclusions seem justified in light of the findings reported here:

- The addition of silica in the composition prevents the anatase to rutile phase transformation even up to 900°C.
- By increasing the boron oxide in the composition, the viscosity of the system decreases, so the crystallinity of the glass ceramic increases.
- With the increase of boron oxide from 5 to 15% by weight (in the constant weight percentage of silica), anatase crystallised in the system as a single phase.
- Following 60 minutes of UV irradiation, the decomposition rate of methylene blue in the synthesised glass ceramic coating can reach up to 30%.

REFERENCES

- [1] Rajesh Kumar, S., Suresh C., Vasudevan A.K., Suja N.R., Mukundan P. and Warriar K.G.K., "Phase transformation in sol-gel titania containing silica". *Mater. Lett.*, 1999, 38, 161-166.

- [2] Fujishima A., Zhang X. and Tryk D.A., "TiO₂ photocatalysis and related surface phenomena". *Surf. Sci. Rep.* 2008, 63, 515–82.
- [3] Tajer-Kajinebaf V., Sarpoolaky H. and Mohammadi T., "Sol-gel synthesis of nanostructured titania-silica mesoporous membranes with photo-degradation and physical separation capacities for water purification". *Ceram. Int.*, 2014, 40, 1747–1757.
- [4] Cheng P., Zheng M., Jin Y., Huang Q. and Gu M., "Preparation and characterization of silica-doped titania photocatalyst through the sol-gel method". *Mate. Lett.*, 2003, 57, 2989–2994.
- [5] Li Zh., Hou B., Xu Y., Wu D., Sun Y., Hu W. and Deng F., "Comparative study of sol-gel hydrothermal and sol-gel synthesis of titania-silica composite nanoparticles". *J. of solid state chem.*, 2005, 178, 1395–1405.
- [6] Bosc F., Ayrat A., Albouy P.A. and Guizard C., "A simple route for low- temperature synthesis of mesoporous and nanocrystalline anatase thin films". *Chem. Mat.*, 2003, 15, 2463–2468.
- [7] Jung K. Y., Park S. B. and Ihm S. K., "Local structure and photocatalytic activity of B₂O₃–SiO₂/TiO₂ ternary mixed oxides prepared by sol–gel method". *Appl. Catal. B: Environ.*, 2004, 51, 239–245.
- [8] Iordanova R., Gegova R., Bachvarova-Nedelcheva A. and Dimitriev Y., "Sol-gel synthesis of composites in the ternary TiO₂–TeO₂–B₂O₃ system". *Phys. Chem. Glasses: Eur. J. Glass Sci. Technol. B*, 2015, 56 (4), 128–138.
- [9] Moon S. C., Mametsuka H., Suzuki E., and Nakahara Y., "Characterization of titanium-boron binary oxides and their photocatalytic activity for stoichiometric decomposition of water". *Catal. Today*, 1998, 45, 79–84.
- [10] Jung K.Y. and Park S.B., "Anatase-phase titania: preparation by embedding silica and photocatalytic activity for the decomposition of trichloroethylene". *J. Photochem. Photobiol. A*, 1999, 127, 117–122.
- [11] Ijadpanah-Saravia H., Zolfagharib M., Khodadadic A. and Drogui P. "Synthesis, characterization, and photocatalytic activity of TiO₂–SiO₂ nanocomposites". *Desalin. Water Treat.*, 2016, 57, 14647–14655.
- [12] Anderson C. and Brad A.J., "Improved Photocatalytic Activity and Characterization of Mixed TiO₂/SiO₂ and TiO₂/Al₂O₃ Materials". *J. Phys. Chem. B*, 1997, 101, 2611–2616.
- [13] Li Z., Hou B., Xu Y., Wu D. and Sun Y., "Hydrothermal synthesis, characterization, and photocatalytic performance of silica-modified titanium dioxide nanoparticles". *J. Colloid Interface Sci.*, 2005, 149–154.
- [14] Bayram B., "Photocatalytic Activity of Titania–Silica Mixed Oxides Prepared with Co-Hydrolyzatio", M.S. Thesis in Chemical Engineering Department, Middle East Technical University.
- [15] Resende S. F., Gouveia R. L., Oliveira B. S., Vasconcelos W. L. and Augusti R., "Synthesis of TiO₂/SiO₂–B₂O₃ Ternary Nanocomposites: Influence of Interfacial Properties on their Photocatalytic Activities with High Resolution Mass Spectrometry Monitoring". *J. Braz. Chem. Soc.*, 2017, 28 (10), 1995–2003.
- [16] Bachvarova-Nedelcheva, A., Iordanova, R., Stoyanova, A., Georgieva, N., Nemska V. and Foteva T., "Effect of B₂O₃ on the Structure, Properties and Antibacterial Abilities of Sol-Gel-Derived TiO₂/TeO₂/B₂O₃ Powders". *Materials*, 2023, 16, 6400.
- [17] Sciancalepore C. and Bondioli F., "Durability of SiO₂–TiO₂ photocatalytic coatings on ceramic tiles". *Int. J. Appl. Ceram. Technol.*, 2015, 12, 679–684.
- [18] Fu J., "Highly photocatalytic glass ceramics containing MgTi₄(PO₄)₆ crystals". *Mater. Lett.*, 2014, 118, 84–87.
- [19] Beall GH, Pinckney LR. Nanophase glass–ceramics. *J. Am. Ceram. Soc.* 1999; 82: 5–16.
- [20] Masai H., Fujiwara T. and Mori H., "Fabrication of TiO₂ nanocrystallized glass". *Appl. Phys. Lett.*, 2007, 90, 081907 (3).
- [21] Yazawa T., Machida F., Oki K., Mineshige A. and Kobune M., "Novel porous TiO₂ glass ceramics with highly photocatalytic ability". *Ceram. Int.*, 2009, 35, 1693–7.
- [22] Fu J., "Photocatalytic properties of glass ceramics containing anatase-type TiO₂". *Mater. Lett.*, 2012, 68, 419–22.
- [23] Fu J., "Photocatalytic activity of glass

- ceramics containing Nasicon-type crystals”. *Mater. Res. Bull.*, 2013, 48, 70–3.
- [24] D. D. Mulmi, D. Thapa, B. Dahal, D. Baral, P. R. Solanki, “Spectroscopic Studies of Boron Doped Titanium Dioxide Nanoparticles”. *IJMSE*, 2016, 3, 172-178.
- [25] Cano-Casanova L., Ansón-Casaos A., Hernández-Ferrer J., Benito A. M., Maser W. K., Garro N., Lillo-Ródenas M. A. and, Román-Martínez M. C., “Surface-Enriched Boron-Doped TiO₂ Nanoparticles as Photocatalysts for Propene Oxidation”. *ACS Appl. Nano Mater.*, 2022, 5, 9, 12527-12539.
- [26] Zhang J., Zhang Y., Leia Y., and Pan C., “Photocatalytic and degradation mechanisms of anatase TiO₂: a HRTEM study.” *Catal. Sci. Technol.*, 2011, 1, 273–278.
- [27] Desch N., Rheindorf A., Fassbender C., Sloot M. and Lak M., “Photocatalytic degradation of methylene blue by anatase TiO₂ coating”. *Appl. Res.*, 2024, 3, e202300081.